Journal of Electroceramics, 13, 55–63, 2004

Platinum (100) Hillock Growth in Pt/Ti Electrode Stack for $SrBi_2Ta_2O_9$ Ferroelectric Random Access Memory

WON WOONG JUNG,*[,1] SI KYUNG CHOI,[1] SOON YONG KWEON[2] & SEUNG JIN YEOM[3]

[1]*Department of Materials Science and Engineering, Korea Advanced Institute of Science and Technology, 373-1 Kusong-Dong, Yusung-Gu, Daejeon 305–701, South Korea*

[2]*Department of Materials Science and Engineering, Chungju National University, 123 Gumdan-ri, Iryumyeon, Chungju, Chungbuk 380-702, South Korea*

[3]*Memory Research and Development Division, Hynix Semiconductor Inc., San 136-1, Ami-ri, Bubal-eub, Ichon-si, Kyoungki-do 467-701, South Korea*

Submitted February 11, 2003; Revised February 3, 2004; Accepted February 4, 2004

Abstract. The ferroelectric material $SrBi_2Ta_2O_9$ (SBT) has been extensively investigated in connection with integrating nonvolatile ferroelectric random-access memory (FeRAM). The SBT layer must be annealed in an oxygen atmosphere after deposition to crystallize the ferroelectric oxide film, which induces Pt hillock formation in a Pt/Ti electrode stack. The Pt hillock in a Pt/Ti electrode stack has been the main concern in SBT FeRAM due to reliability problems, such as capacitor shorts.Reportedly, the compressive stress generated in thin film is widely accepted as being responsible for the occurrence of hillocks in thin film and the main mass transport mechanism for hillock formation is the grain boundary diffusion for thin film with a columnar structure. In this study, three factors are considered in the total compressive stress generated during both deposition and post-annealing in Pt/Ti electrode stack: intrinsic stress, thermal stress, and extrinsic stress. Moreover, we found that an orientation relationship of Pt $(100)_{\text{hillock}}$//Pt $(111)_{\text{thin film}}$ existed between the Pt hillock and the thin film. The Pt hillock was a single crystal, having facets with polyatomic steps. From these results, we suggest that the Pt hillock growth mechanism is the layer growth of flat faces, which shapes the hillock into a tetrahedron single crystal.

Keywords: FeRAM, hillock, stress, facet, single crystal

1. Introduction

Ferroelectric $SrBi_2Ta_2O_9$ (SBT) thin films have many advantages when compared to $Pb(Zr_xTi_{1-x})O_3$ (PZT) thin films, such as a fatigue-free, low leakage current, and stable imprint characteristics for the application of ferroelectric random access memory (FeRAM) [1, 2]. In addition, the Pt is chemically stable in a high processing temperature, which is necessary for crystallizing the ferroelectric oxide film. However, the adhesion of Pt to substrates such as silicon-oxide (SiO_x) is poor [3]. Therefore, a Ti glue layer has typically been employed.

The Pt/Ti electrode stack deposited by the sputtering method tends to have a significant instability problem, i.e., Pt hillock formation. Pt hillocks are a major concern because they can lead to capacitor shorts, as reported previously [4, 5]. It has been reported that hillock formation depends strongly on the compressive stress generated during both sample preparation and post-annealing [6, 7] and that the main mass transport mechanism for the growth of the hillock on the thin film with a columnar structure is the grain boundary diffusion [8, 9]. Three factors are considered in the total compressive stress of the Pt/Ti electrode stack: intrinsic stress, thermal stress, and extrinsic stress [4, 5].

Among the three factors, intrinsic stress and extrinsic stress are most important in device integration since the stress values of theses two factors are relatively higher than the value of thermal stress. The values of intrinsic stress and extrinsic stress can be easily adjusted with the process parameters and sequence [4, 5]. There have been few systematic investigations, however, of the relationship between Pt hillock formation

*To whom all correspondence should be addressed. E-mail: cww2000@kaist.ac.kr

and stresses in the Pt/Ti electrode stacks, and there have been few reports on the orientation relationship between the Pt hillock and Pt thin film. In this study, we report the results of the stress dependence of Pt hillock formation on the Pt surface during post thermal cycling, and we report the orientation relationship between the Pt hillock and the thin film to be $Pt(100)_{hillock}//Pt(111)_{thin\ film}$, We also make a suggestion regarding the hillock growth mechanism.

2. Experimental Procedure

Both Pt and Ti films were sputter-deposited on a ⟨100⟩-oriented 8-inch silicon substrate, passivated with a thermally grown SiO_x layer of 1000 Å thickness. The respective thicknesses of Pt and Ti were 2000 Å (sputtering rate 40 Å /s) and 200 Å (sputtering rate 10 Å /s). The details for the fabrication of the Pt/Ti electrode stack can be found in the literature [4, 5]. The electrode stacks were annealed in the diffusion furnace, from room temperature (RT) to 650°C in an oxygen atmosphere. The SBT film of about 1500 Å thickness was deposited using a spin-on method with a metalorganic decomposition (MOD) solution. After baking and rapid thermal annealing steps, the films were annealed at 800°C in oxygen ambient for ferroelectric crystallization. It should be noted that the patterning process of the SBT capacitor was described elsewhere in detail [4, 5].

Stress-temperature curves were obtained during the annealing process using a stress measurement system (FLX-2908, TENCOR). The ferroelectric properties of SBT capacitors were measured in a 50 μm × 50 μm large pattern using a RT6000SI ferroelectric tester (Radiant Technologies Co.). Scanning electron microscopy (SEM) and in situ high temperature X-ray diffraction (XRD) were used to analyze Pt hillock formation at various annealing temperatures. To clarify the orientation relationship between the Pt hillock and the thin film, cross-sectional images of high-resolution transmission electron microscopy (HRTEM) were captured with a Philips F-20 at 200 kV.

3. Results and Discussion

3.1. The Origin of Pt Hillock Formation in the Pt/Ti Electrode Stack

Figure 1 shows the Pt hillocks formed on a Pt/Ti stack as a function of annealing temperature, where the Pt layer was deposited at RT on Ti films. Notice that the height of hillocks observed on the sample annealed at 650°C is in the same range (and even higher) as the typical thickness of a ferroelectric thin film used in FeRAM (about 200 nm), which explains why the formation of Pt hillock in the bottom electrodes of FeRAM capacitors is a major concern, especially with regard to such problems as capacitor shorts.

We analyzed the stress-temperature curves measured by FLX-2908 to explain the relationship between the compressive stress and hillock formation. The stress of Pt/Ti electrode stacks changes during thermal cycling as illustrated in Fig. 2. The initial stress (marked 'A' in Fig. 2(a)) of the Pt film deposited at RT is in a compressive stress state. In contrast, the Pt film deposited at 500°C shows the state of tensile stress (marked 'F' in Fig. 2(b)). Reportedly, these compressive and tensile stresses are collectively defined to be intrinsic stress [4], which is dependent on the deposition temperature of the Pt layer. After this intrinsic stress, the thermal compressive stress ('A-B' segment in Fig. 2(a)) increased proportionally and all of these compressive stresses amount to a large stress value of about -10×10^9 dyne/cm^2 (marked 'B' in Fig. 2(a)). This value of compressive stress in the Pt/Ti electrode stack during annealing is too large to retain in the Pt layer. Accordingly, the Pt hillock is formed in the Pt/Ti electrode stack to relieve this large compressive stress [4, 6, 7]. The initial state of hillocks appeared at an annealing temperature of below 500°C as shown in Fig. (1), after the relaxation (marked 'B-C' segment in Fig. 2(a)) of thermal and intrinsic compressive stresses finished. We perceived that the intrinsic stress is dependent on the deposition temperature of the Pt layer and that this intrinsic stress provided the cause for the initial state of Pt hillock formation.

A closer look at Fig. 2(a) shows that the slope of the C-D segment is different from that of the A-B segment. We can suspect that this difference was caused by another stress (C-D segment) aside from intrinsic and thermal stresses. Figure 2(c) shows that the curve obtained in the Pt film directly on the SiO_x/Si substrate without a Ti glue layer has no variation of the slope for the range of heating. No variation of the slope in the curve means that only thermal compressive stress contributes to the total compressive stress, which indicates that the origin of another stress is related to the Pt and Ti interactions during the post-annealing process, after Pt deposition. Note that the Pt deposition temperature

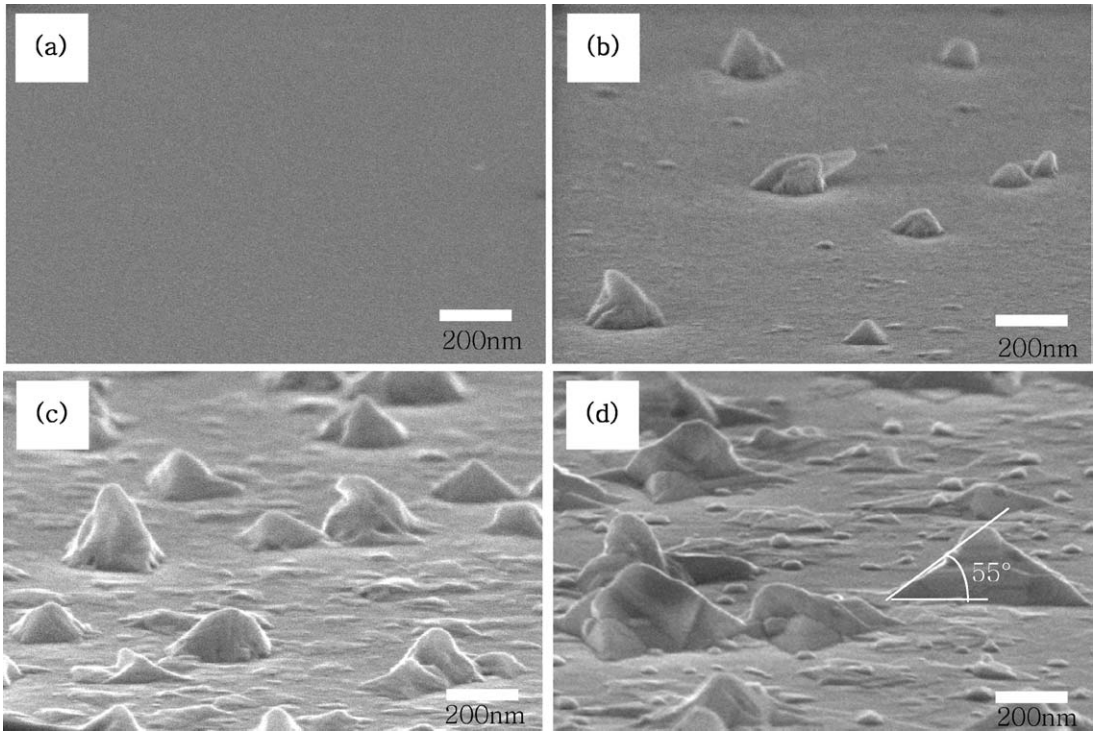

Fig. 1. The side-view SEM micrographs of hillocks in the Pt/Ti electrode stack after annealing, in which Pt was deposited at RT on Ti films. The annealing temperature was (a) 450°C, (b) 500°C, (c) 600°C and (d) 650°C. The angle between the basal plane and facet of the hillock is about 55°, as indicated in (d).

was 500°C, to exclude the effect of intrinsic compressive stress in this experiment.

To obtain the proof of the Pt and Ti interactions, a cross-sectional TEM image was observed of the Pt/Ti electrode stacks annealed at various temperatures, as shown in Fig. 3. The Pt/Ti interface remains smooth at the annealing temperature up to 400°C as shown in Figs. 3(a) and (b). As Pt and Ti interdiffusion increased above 500°C, however, the interfacial boundary collapsed. Some compounds formed by the interdiffusion were observed along the Pt grain boundaries and the interface Pt and Ti layer. An energy-dispersive spectroscopy (EDS) analysis (e-beam size: 20 nm) was performed during the TEM analysis to trace the elements of the compounds as shown in Fig. 3(d). Ti, oxygen, and Pt were detected at the points marked 'A' and 'B', but only Pt was detected at point 'C'. Also, TiO_x grains were found along Pt grain boundaries.

The Pt and Ti compound formed along the interface of Pt and Ti layer, but was not observed at the Pt grain boundaries. We believe that this Pt and Ti compound had no effect on the evolution of the compressive stress in the Pt layer. On the other hand, the Ti diffused into the Pt layer along the grain boundaries and was oxidized at the grain boundaries during the annealing in an oxygen atmosphere due to the fact that Ti has a higher affinity for oxygen than Pt does. This Ti oxidation phenomenon induces the compressive stress in the Pt layer by the volume expansion ($Ti \rightarrow TiO_x$).

Given the above result, another compressive stress (C-D segment in Fig. 2(a)) aside from intrinsic stress and thermal stress in the Pt layer is considered to be an additional external compressive stress. This external compressive stress (approximately -11×10^9 dyne/cm^2) is the largest compressive stress in among the compressive stresses as shown in Fig. 2(a), which causes the Pt hillock to be mature and larger. That is, it was the major driving force behind the formation of the larger Pt hillock.

Figure 4 illustrates *P-E* hysteresis loops of the SBT capacitor deposited on Pt/Ti electrode stacks at RT and 500°C of the Pt deposition temperatures. To obtain *P-E* hysteresis loops of the SBT capacitor, the

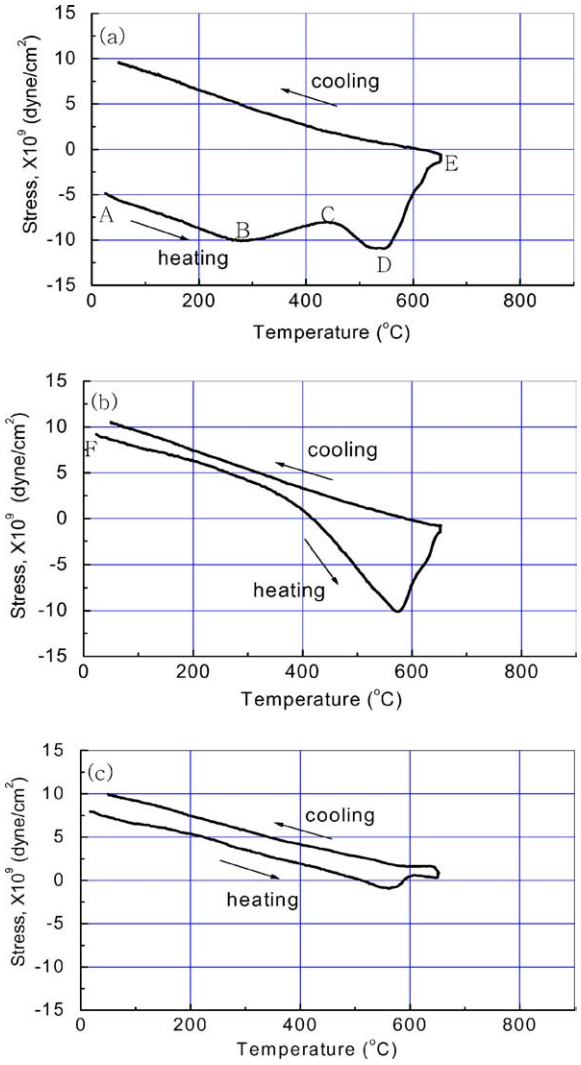

Fig. 2. The stress-temperature curves obtained at the Pt/Ti electrodes deposited on SiO_x/Si substrate. The deposition temperatures of the Pt layers were (a) RT, (b) 500°C, and (c) Pt films were deposited at 500°C directly on SiO_x/Si without a Ti glue layer.

SBT capacitor should be annealed at 800°C in oxygen ambient for ferroelectric crystallization, which is the cause of Pt hillock formation. All of the SBT capacitors on Pt films deposited at RT exhibited short failure (100%). In contrast, there were no short failures in the SBT capacitors when Pt films were deposited at 500°C. These results are well consistent with the trend of the intrinsic compressive stress evolution. The compressive stress dependence of Pt hillock formation surely affected the *P-E* hysteresis loops of the SBT capacitor.

3.2. Platinum (100) Hillock Growth Mechanism

Most of the hillocks appear to be nano-sized tetrahedrons as shown in Fig. 1. The angle between the basal plane and the facet of the tetrahedron was observed at about 55°, as shown in Fig. 1(d). Since the interplanar angle in cubic crystals between {100} and {111} plane is 54.7°, we easily inferred that the facet of the tetrahedron-shaped Pt hillock was the (111) plane for the surface energy minimum. This phenomenon means that the basal plane and the stacked plane should be (100) plane.

The XRD profiles of the Pt/Ti electrode stack annealed at 650°C, as shown in Fig. 5(a), reveal a new Pt (200) peak, which was absent in as-deposited Pt/Ti electrode stack. The Pt thin film electrode had a ⟨111⟩ preferred orientation, confirming that the Pt (200) peak originates from the stacked plane of a tetrahedron-shaped Pt hillock, which is assumed to be the Pt (100) plane, as mentioned above. The in situ high temperature XRD measurement, as shown in Fig. 5(b), reveals that the Pt (200) peak increases as a function of the annealing temperature and Pt hillock size also increases as a function of the annealing temperature, as shown in Fig. 1. Therefore, we can exclude the possibility of the Pt (200) peak, as shown in Fig. 5(a), arising from the recrystallized grain or the grain growth of the Pt thin film during electrode annealing. The Pt hillock clearly has a ⟨100⟩ orientation against a ⟨111⟩ preferred orientation of Pt thin film, as shown in Figs. 5(a) and (b).

Figure 6(a) shows a micro-diffraction pattern obtained from a Pt hillock. This result implies that the Pt hillock is a single crystal and its formation is based on a single crystal growth mechanism. Cross-sectional HRTEM images of the hillock and the thin film area were separately acquired with the same [011] beam direction, as shown in Figs. 6(b) and (c), respectively. The insets show the diffraction patterns simulated from the corresponding HRTEM image. As shown in Figs. 6(b) and (c), the Pt hillock and thin film clearly have different orientations ($Pt\langle 100\rangle_{hillock}$//$Pt\langle 111\rangle_{thin\ film}$), which coincide with the results of the XRD data. A closer look at Fig. 6(b) shows that the Pt hillock has a ⟨100⟩ orientation and {111} facets that are inclined at 54.7° to the {100} planes to minimize surface energy.

Figure 7(a) shows a typical tetrahedron-shaped Pt hillock observed in a Pt/Ti stack annealed at 650°C in oxygen atmosphere. Since the average diameter of the Pt fiber is about 50 nm, measured by a plane-view

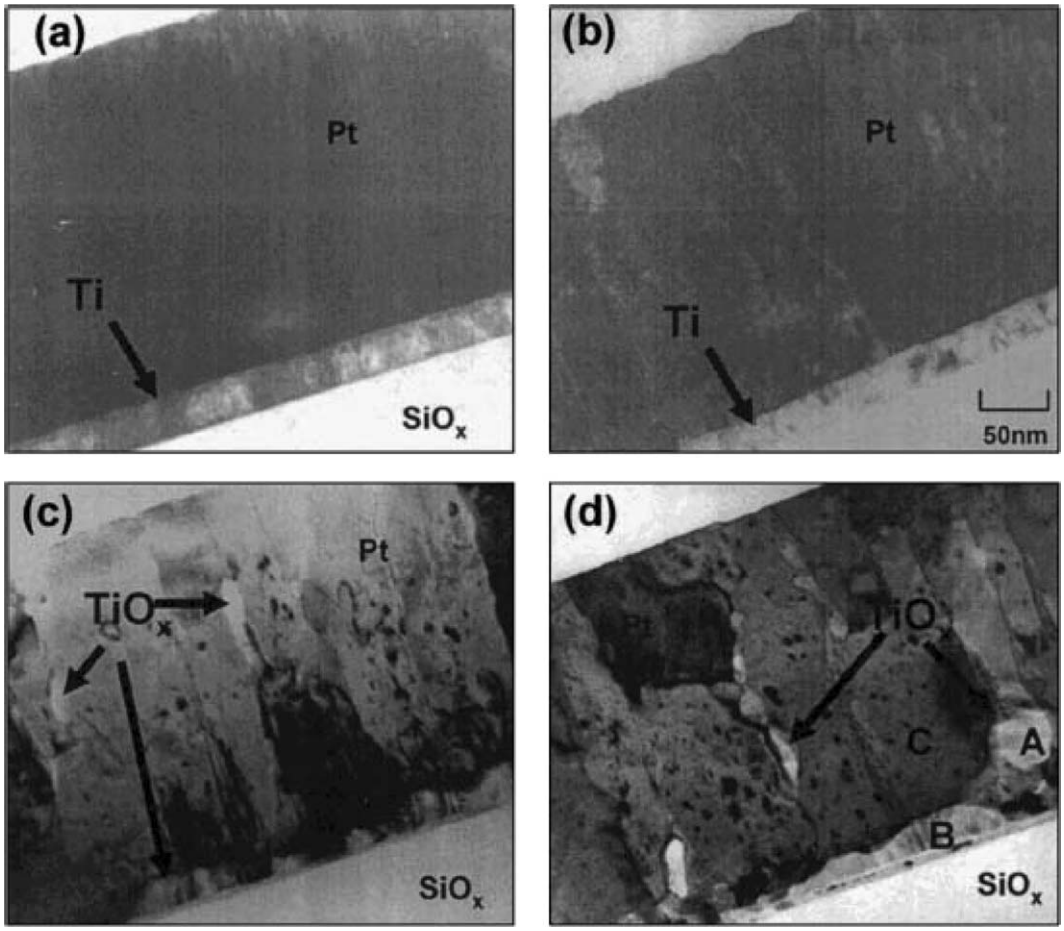

Fig. 3. Cross-sectional TEM images observed in the Pt/Ti electrode stacks annealed at various temperatures: (a) RT, (b) 400°C, (c) 500°C, and (d) 600°C, where the Pt layer was deposited at RT.

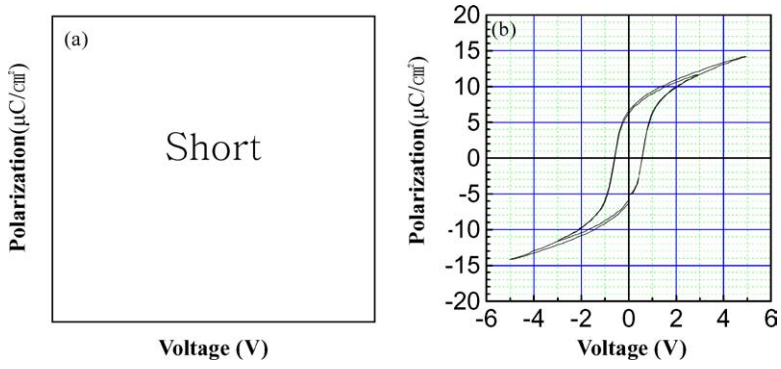

Fig. 4. Polarization vs. voltage (*P-E*) hysteresis loops of the SBT capacitors deposited on Pt/Ti electrode stacks. The deposition temperatures of the Pt films were (a) RT, and (b) 500°C, where the SBT capacitors were annealed at 800°C in oxygen ambient for ferroelectric crystallization.

image of SEM as shown in Fig. 7(a), the interface area of the hillock is much larger than the cross-sectional area of the Pt fiber. In the Pt/Ti electrode stack, the Pt hillock formation is due to the relaxation process of the compressive stress in the film; the Pt atoms move to the film surface from the interior along the grain boundary. Therefore, at the initial state of the Pt hillock, the mass for its growth is supplied by grain boundary diffusion [8, 9]. However, for the large hillock shown in Fig. 7(a), the movement of the Pt atoms along the grain boundaries underneath the hillock can not directly contribute to the hillock growth because the interface between the hillock and the film blocks the diffusion of the Pt atoms toward the facets of hillock.

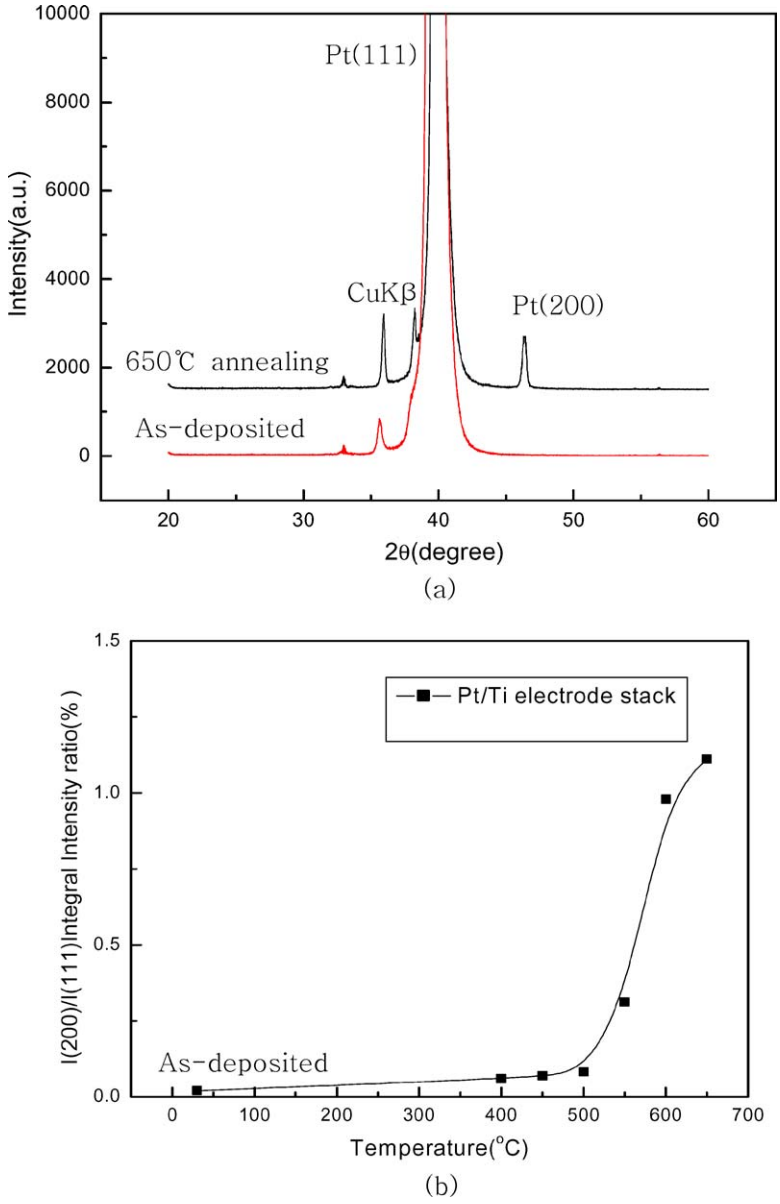

Fig. 5. (a) The X-ray diffraction pattern of a Pt/Ti electrode stack at as-deposited and 650°C annealing temperature. (b) The $I_{(200)}/I_{(111)}$ peak integral intensity ratio of the Pt/Ti electrode stack according to temperature changes obtained by an in situ high temperature X-ray diffraction measurement.

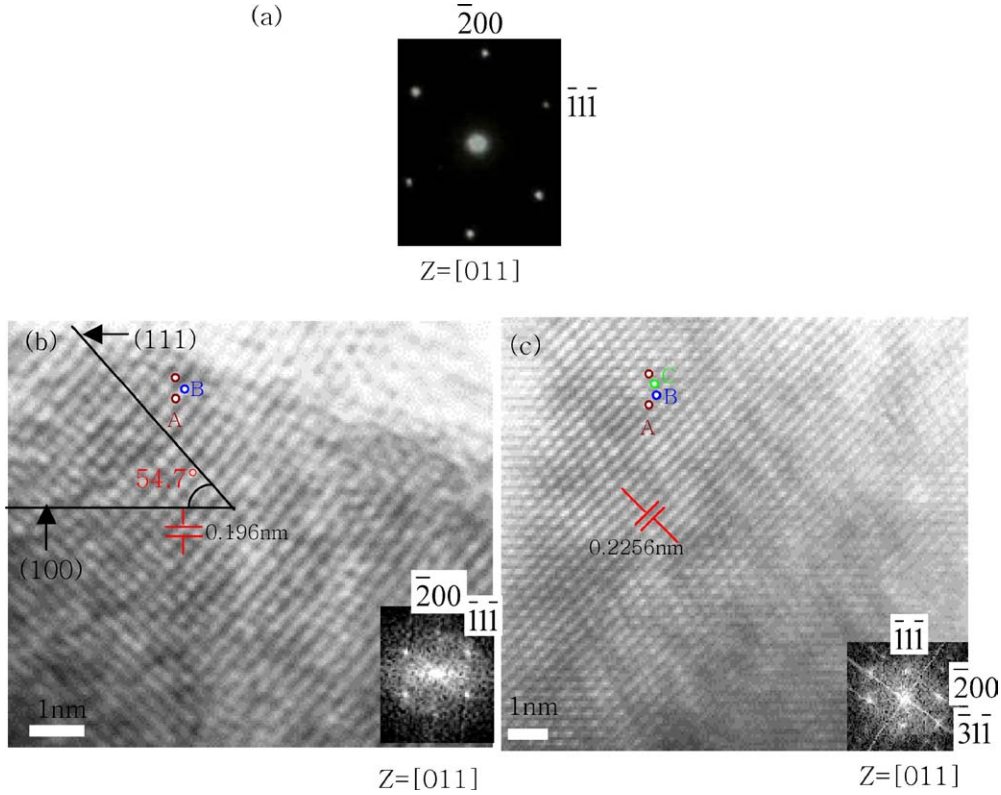

Fig. 6. (a) The micro-diffraction pattern obtained from a Pt hillock. The cross-sectional HRTEM image of (b) Pt hillock, and (c) Pt thin film, observed with the same [011] beam direction. The inset to (b) and (c) is a diffraction pattern simulated from respective HRTEM images.

We can clearly find the polyatomic steps on the facets of the large Pt hillock, as shown in Fig. 7(a); and the behavior of the Pt (200) peak in Fig. 5(b) shows that the Pt hillocks grow with a ⟨100⟩ orientation as a function of annealing temperature. These results have led to our suggestion on the growth mechanism of the large hillock, as seen in Figs. 1(b)–(d); the large hillock is the layer growth of flat faces represented in Fig. 7(b) [10]. Above 500°C, the Pt layer was in a large compressive stress of about -11×10^9 dyne/cm^2 as shown in Fig. 2(a). This stress resulted from the Ti diffusion into Pt layer and its oxidation (TiO_x) in the Pt grain boundary. However, Ti atoms did not diffuse out to the (111) Pt surface. Below 500°C, such a large compressive stress did not form due to less Ti diffusion into the Pt layer. The diffusion of Pt atoms along the grain boundary occurred actively toward the film surface to relax the strong compressive stress [11]. The Pt atoms on the film surface, which was diffused out from the interior, departed toward the hillock along the film surface and afterwards accumulated just around the hillock. Accordingly, a gradient of the diffused-out Pt atoms exists between the steps of facets in the hillock, as illustrated in Fig. 7(b). Due to this gradient, more Pt atoms have a chance of jumping up to the upper layer along the {111} facets; they subsequently form a new upper layer until the concentration gradient vanishes.

4. Summary

The deposition temperature dependence of Pt hillock formation could be explained by the difference in the intrinsic compressive stress generated during deposition process. Ti diffusion into the Pt layer started at the annealing temperature of about 400°C along the Pt grain boundaries in the Pt/Ti electrode stacks and the Ti in the Pt layer was oxidized during the post-annealing process in oxygen atmosphere. The large hillocks (200 nm) could be observed on Pt surface annealed at above 500°C. It was clear that the highest

extrinsic compressive stress (approximately -11×10^9 dyne/cm^2) generated by Ti diffusion into the Pt layer followed by oxidation was the major driving force for the large hillock formation. Therefore, the origin of the Pt hillock formation in Pt/Ti electrode stack is considered to be intrinsic, thermal and extrinsic compressive stress.

We also found that the Pt hillock was a single crystal with an orientation relationship of $Pt(100)_{hillock}//Pt(111)_{thin\ film}$ between the Pt hillock and the thin film. It is proposed that the Pt hillock grows as a result of the layer growth of flat faces, which shape the hillock into a tetrahedron single crystal.

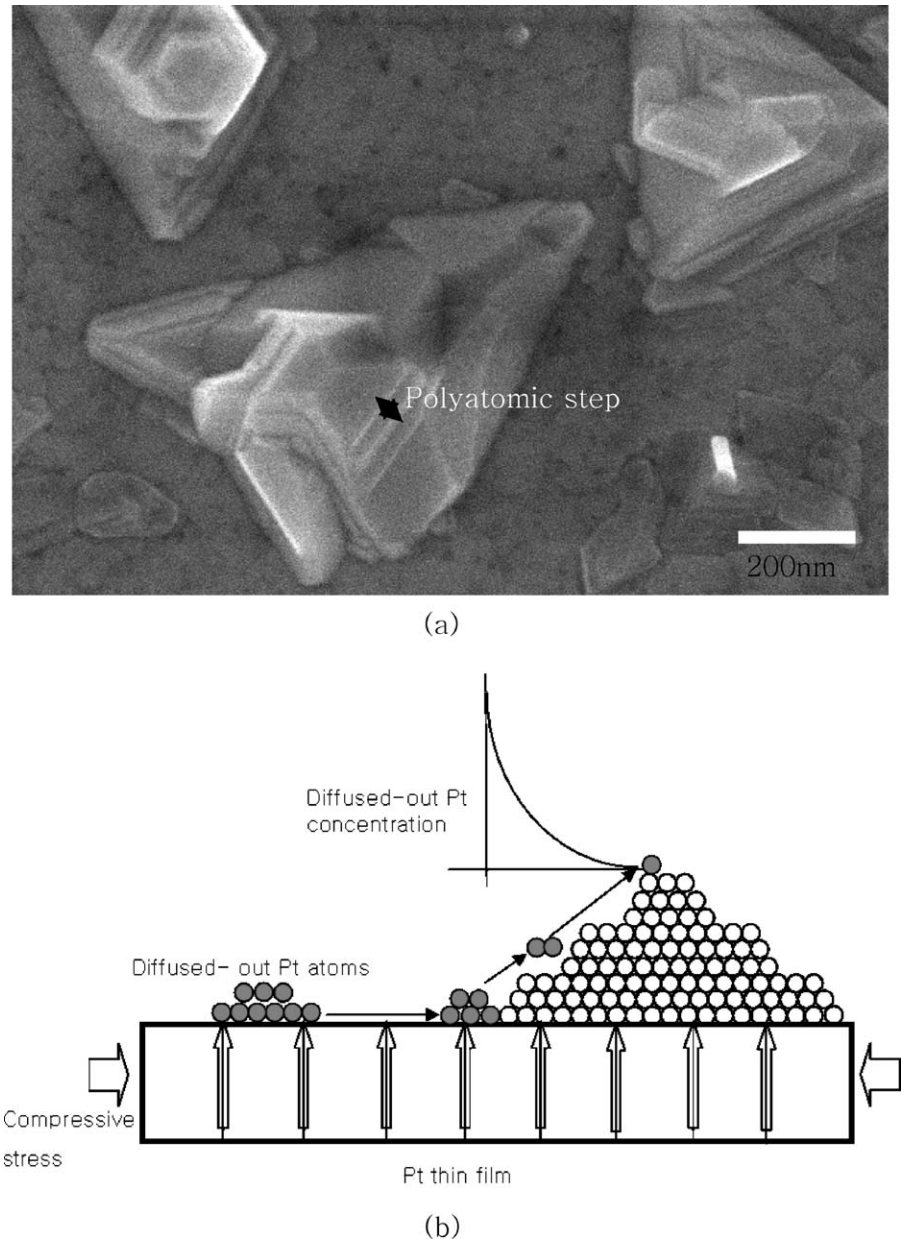

Fig. 7. (a) Plane-view SEM image of a Pt hillock showing polyatomic steps. (b) Schematic diagram of the layer growth of flat faces in a large Pt hillock, with a cross-sectional view.

Acknowledgment

This work was supported by grant no. R01-2000-00226 from the basic research program of the Korea Science & Engineering Foundation. It was also supported by the Brain Korea 21 project in 2003 and the Ministry of Science and Technology (M1010500066-01H2006400).

References

1. C.A. Paz de Araujo, J.D. Cuchiaro, L.D. McMillan, M.C. Scott, and J.F. Scott, *Nature*, **374**, 627 (1995).
2. T. Mihara, H. Yoshimori, H. Watanabe, and C.A. Paz de Araujo, *Jpn. J. Appl. Phys.*, **34**(9B), 5233 (1995).
3. I. Kondo, T. Yoneyama, and O. Takenaka, *J. Vac. Sci. Technol. A*, **10**, 3456 (1992).
4. S.Y. Kweon, S.J. Yeon, H.J. Sun, N.K. Kim, Y.S. Yu, and S.K. Lee, *Integrated Ferroelectrics*, **25**, 299 (1999).
5. S.Y. Kweon, S.K. Choi, S.J. Yeom, and J.S. Roh, *Jpn. J. Appl. Phys.*, **40**, 5850 (2001).
6. S.K. Lahiri and O.C. Wells, *Appl. Phys. Lett.*, **15**, 234 (1969).
7. W.B. Pennebaker, *J. Appl. Phys.*, **40**, 394 (1969).
8. P. Chaudhari, *IBM J. Res. Dev.*, **13**, 197 (1969).
9. E. Iwamura, T. Ohnishi, and K. Yoshikawa, *Thin Solid Films*, **270**, 450 (1995).
10. I.V. Markov, *Crystal Growth for Beginners* (World Scientific Publishing, 1995), p. 155.
11. E. Chason, B.W. Sheldon, L.B. Freund, J.A. Floro, and S.J. Hearne, *Phys. Rev. Lett.*, **88**, 16103 (2002).